

C-Arm Computed Tomography Compared With Positron Emission Tomography/Computed Tomography for Treatment Planning Before Radioembolization

Christoph Becker · Tobias Wiggershauser · Reinhold Tiling · Sabine Weckbach · Thorsten Johnson · Oliver Meissner · Klaus Klingenberg-Regn · Maximilian Reiser · Ralf Thorsten Hoffmann

Received: 16 March 2010 / Accepted: 10 May 2010 / Published online: 29 May 2010
© Springer Science+Business Media, LLC and the Cardiovascular and Interventional Radiological Society of Europe (CIRSE) 2010

Abstract The purpose of this study was to determine whether rotational C-arm computed tomography (CT) allows visualization of liver metastases and adds relevant information for radioembolization (RE) treatment planning. Technetium angiography, together with C-arm CT, was performed in 47 patients to determine the feasibility for RE. C-arm CT images were compared with positron emission tomography (PET)/CT images for the detection of liver tumors. The images were also rated according one of the following three categories: (1) images that provide no additional information compared with DSA alone; (2) images that do provide additional information compared with DSA; and (2) images that had an impact on eligibility determination for and planning of the RE procedure. In all patients, 283 FDG-positive liver lesions were detected by PET. In venous contrast-phase CT, 221 (78.1%) and 15 (5.3%) of these lesions were either hypodense or hyperdense, respectively. In C-arm CT, 103 (36.4%) liver lesions were not detectable because they were outside of either the field of view or the contrast-enhanced liver segment. Another 25 (8.8%) and 98 (34.6%) of the liver lesions were either hyperdense or presented primarily as hypodense lesions with a rim enhancement, respectively. With PET/CT

as the standard of reference, venous CT and C-arm CT failed to detect 47 (16.6%) and 57 (20.1%) of all liver lesions, respectively. For RE planning, C-arm CT provided no further information, provide some additional information, or had an impact on the procedure in 20 (42.5%), 15 (31.9%) and 12 (25.6%) of patients, respectively. We conclude that C-arm CT may add decisive information in patients scheduled for RE.

Keywords Interventional radiology · Complication · Tumor seeding

Introduction

In its current approach, radioembolization (RE), also known as selective internal radiation therapy, is a relatively new therapeutic option in patients with nonresectable liver metastases [1]. By injecting ⁹⁰Yttrium (Y-90)-embedded resin [2] or glass microspheres directly into the hepatic arteries, a high dose of beta radiation can be administered selectively to the tumor site. In preparation for RE, diagnostic invasive angiography is the initial step to assess first- and second-order anatomy and variations of the hepatic arteries [3]. Selective catheterization of the left and right hepatic branches is mandatory to assess blood flow and to identify smaller side branches, such as the falciform artery, the right phrenic artery, or the accessory gastric, supraduodenal or retroduodenal, or cystic arteries. Otherwise, Y-90 microspheres may embolize into unrecognized collateral vessels and result in gastrointestinal tract toxicities, including gastroduodenal ulceration, pancreatitis, cholecystitis, and esophagitis [4].

Pre-RE evaluation also includes injection of ^{99m}Tc-macroaggregated albumin (Tc-MAA) through the

C. Becker (✉) · T. Wiggershauser · S. Weckbach · T. Johnson · M. Reiser · R. T. Hoffmann
Department of Clinical Radiology, Ludwig-Maximilians-University Hospital, 81377 Munich, Germany
e-mail: christoph.becker@med.uni-muenchen.de

R. Tiling
Clinic of Nuclear Medicine, Ludwig-Maximilians-University Hospital, 81377 Munich, Germany

O. Meissner · K. Klingenberg-Regn
Siemens AG Healthcare Sector, 91301 Forchheim, Germany

angiography catheter into the right and left hepatic arteries primarily to calculate the required Y-90 activity and to exclude pulmonary shunting, which could potentially cause radiation pneumonitis subsequent to RE. Extrahepatic gastrointestinal uptake, which may be the result of an unrecognized hepato-fugal runoff, may also be detected using Tc-MAA scintigraphy [5].

Rotational C-arm computed tomography (CT) is a relatively new method that allows intraprocedural reconstruction of CT-like images from projections acquired during a 200° rotation of the C-arm around the patient [6]. In the present study, we sought to determine the ability of C-arm CT to display liver metastases compared with positron emission tomography (PET)/CT and to investigate its value for the work-up of patients in preparation for RE.

Materials and Methods

Diagnostic angiography, C-arm CT, and PET/CT were performed in 47 patients (mean age 61.9 ± 11.1 years; 27 female) for the eligibility and feasibility of RE therapy. Before the examination, all patients gave informed consent to undergo the comprehensive diagnostic work-up. Patient disease included metastases of colorectal ($n = 26$), pancreatic ($n = 2$), or breast cancer ($n = 8$); cholangiocellular carcinoma ($n = 3$); unknown primary cancer ($n = 2$); melanoma ($n = 2$); or ovarian, uterus, adrenal gland, or hepatocellular carcinoma (HCC) ($n = 1$ each).

Digital subtraction angiography (DSA) and C-arm CT were performed with a ceiling-mounted, single-plane, digital flat-panel C-arm system (Axiom Artis dTA, software version VB22; Siemens AG, Forchheim, Germany). A 4F catheter sheath (Terumo, Tokyo, Japan) was placed into the right common femoral artery, and a 4F Cobra catheter (Cordis, Roden, The Netherlands) was used to perform nonselective as well as selective DSA of the superior mesenteric artery and the celiac trunk. A 2.8F microcatheter (ProGreat; Terumo) was used to enter the right and left hepatic arteries for selective DSA.

C-arm CT acquisitions were performed as an adjunct to conventional DSA. Depending on the patient's anatomy and the hepatic tumor load, C-arm CT was performed with the tip of the catheter in either the hepatomesenteric trunk, the common artery, or the right or left hepatic artery in 1, 7, 21, and 28 patients, respectively. Nine patients with multisegmental tumor involvement of the liver underwent more than one C-arm CT scan.

C-arm CT images were generated from an 8-second rotational acquisition over an arc of approximately 200° around the patient. Within 8 seconds, 419 projections were recorded and transferred automatically to a dedicated workstation (Leonardo; Siemens AG) immediately after

acquisition. On this workstation, 395 CT images with a slice thickness and increment of 0.48 mm were automatically reconstructed within 3 to 5 minutes. Due to the cone beam geometry of the X-ray fan, the field of view was 23 cm diameter in axial plane, with a range of 8 cm in z-direction.

For contrast enhancement, 10 ml iodinated contrast material (Iomeron 300; Bracco Imaging, Milan, Italy) were mixed with the same amount of saline and injected manually within 10 seconds immediately before the C-arm CT run. This contrast injection protocol was chosen to decrease viscosity and density of the contrast media, to achieve an adequate and homogenous enhancement of the liver parenchyma, and to avoid artifacts arising from hyperdense liver arteries.

PET-CT was performed using a Philips Gemini System (Philips Medical Systems, Eindhoven, The Netherlands). The patients were fasted for at least 6 hours before the examination. Blood glucose levels verified normoglycemia (<120 mg/dl). Two hundred MBq F-18-fluorodeoxyglucose (FDG) were administered intravenously as radioactive tracer. In addition, 20 mg furosemide and 20 mg butylscopolamine were injected to limit nonspecific bowel activity and to decrease radiation exposure of the urinary tract. To exclude extrahepatic tumor spread, PET/CT was performed as a whole-body examination covering the base of the skull to the middle of the femora. Low-dose CT scan for attenuation correction was started 60 min after FDG application, which was followed by acquisition of PET emission data using a three-dimensional mode (3D; 12 bed positions, acquisition time 3 min/bed position, field of view 10 cm). The examination was completed by a diagnostic dual-detector-row CT scan (130 kVp, 130 mA, 2×5 -mm collimation, 8-mm pitch) of the head, thorax, abdomen, and pelvis after intravenous injection of 120 ml contrast material (Ultravist 300; Schering, Berlin, Germany). Reconstruction of the PET data was performed with and without attenuation correction (Ramla 3D algorithm). Afterward, the PET and CT data were fused on demand using Syntegra software (Syntegra; Mirada Solutions, Oxford, UK) with a matrix of 144×144 pixels.

PET images were evaluated separately for regions of increased focal glucose uptake and semiquantitatively with the region-of-interest technique determining the maximum standardized uptake value (SUV). In equivocal findings, an $SUV_{max} > 2.5$ was considered suspicious for malignancy. Tumors were also assessed as either hyperdense or hypodense lesions in the CT image data set acquired in the venous contrast-enhancement phase independent from PET.

C-arm CT images were evaluated for the presence and appearance of any liver lesions compared with the PET/CT images. The images were further analyzed to determine

whether a particular tumor was confined to the contrast-enhanced liver parenchyma or whether any contrast enhancement was present outside the liver, e.g., in the wall of the gall bladder or the stomach.

Two experienced radiologists, each with >15 years of experience in CT (C. B.) and interventional radiology (T. W.), reviewed the cases in common and categorized by consensus the C-arm CT images into one of the following three groups: (1) images that provide no additional information compared with DSA alone; (2) images that do provide additional information compared with DSA; and (2) images that had an impact on eligibility determination for and planning of the RE procedure. Depending on the results of the entire diagnostic work-up, RE was performed in a separate procedure if applicable.

Results

In all 47 patients, a total of 283 liver lesions with an SUV >2.5 were identified by PET. Venous contrast-enhanced CT, detected 221 (78.0%) and 15 (5.3%) of these lesions as either hypodense or hyperdense lesions, respectively. Correspondingly, 47 (16.6%) PET-positive liver lesions were not seen on venous contrast-phase CT images (Fig. 1). One hundred three of the 283 (36.4%) liver lesions detected by PET/CT were found to be located outside the field of view or the contrast-enhanced liver segments of the C-arm CT images. Of the remaining 180 lesions, 25 (8.8%) and 98 (34.6%) were identified as hyperdense lesions or

hypodense lesions with a characteristic hyperattenuating rim, respectively. Although located in the contrast-enhanced liver segment, the remaining 57 (20.1%) liver lesions could not be seen on the C-arm CT images.

According to our rating system, C-arm CT provided no additional information compared with DSA in 20 of 47 (42.5%) patients and provided additional information in another 15 (31.9%) patients. In 5 patients, it could be demonstrated by C-arm CT that the main tumor load could not be reached by the actual catheter position ($n = 4$) or had no tumor blush at all ($n = 1$). The suspicion of an early portal-venous shunting or a small arterial-venous fistula was raised from C-arm CT images in another 2 patients. Contrast-enhancement outside the liver was detected in the wall of the gall bladder or in the stomach in 3 and 2 patients, respectively. Therefore, information achieved by C-arm CT led to a change in therapy planning or eligibility in 12 (25.6%) patients.

Discussion

Resection of solitary liver metastases is known to improve long-term survival. However, only 10–20% of patients with liver metastases are candidates for surgery, and another 20–25% may qualify for radiofrequency ablation or laser ablation, mostly because of the presence of multifocal disease or general contraindications to any of these therapies. Although systemic chemotherapy regimens have been the mainstay of treatment for many years in these patients, the response and survival rates remained unsatisfactory, most likely because of high relapse rates after chemotherapy and the increasing number of nonresponders to different chemotherapeutical regimens [7].

As an alternative technique, infusion of Y-90-radiolabeled microspheres into the hepatic artery delivers effective doses of radiation to multifocal tumor manifestations within the liver while preventing unacceptable damage to normal liver parenchyma. This technique takes advantage of the fact that metastases derive their arterial supply mainly by neoangiogenesis from the systemic arterial system, whereas the normal liver parenchyma largely depends on the portal venous blood supply. The injected particles become trapped in the capillary arterial vessels of the metastases and thus carry the radiation directly to the target. Given Food and Drug Administration approval for colorectal cancer [8] and European conformance (CE) certification for HCC [9] and in the salvage situation, patients with liver metastases originating from a variety of different malignancies [10] may be treated usually with one but sometimes also with several cycles of RE [7].

RE is performed with intra-arterial catheters that are placed directly into the liver arteries. However, even

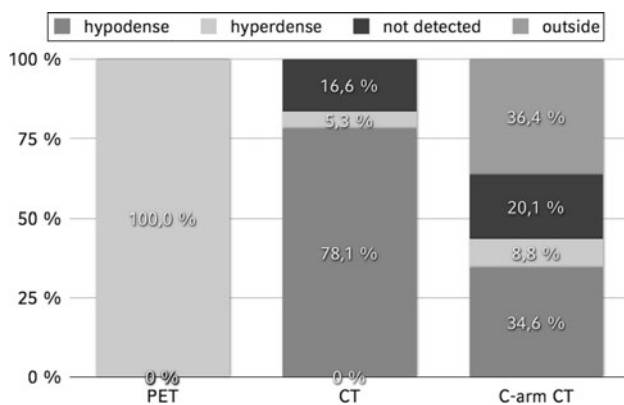


Fig. 1 PET serves as the “gold standard” for the detection of liver lesions. Hypodense and hyperdense liver lesions, 71 and 5.3%, respectively, were detected by venous contrast-phase CT. Of all lesions, 8.8% were hyperdense in C-arm CT, and 34.6% were hypodense, showing a characteristic rim enhancement. Of the liver lesions, 16.6 and 20.1%, respectively, were detected neither by conventional CT nor by C-arm CT. Another 36.4% of all lesions were outside the field of view or the contrast-enhanced liver parenchyma in C-arm CT images

selective placement of the catheter may carry the risk of retrograde or collateral flow and the spread of microspheres to territories other than the primary tumor target in the liver. The most serious complications of RE are gastric or duodenal ulcers, pancreatitis, cholecystitis, and esophagitis resulting from reflux or inadvertent injection of Y-90 microspheres into the gastrointestinal vasculature. Angiography and DSA are of paramount importance in planning administration of the microspheres. If any side branches can be identified, potentially providing extrahepatic structures, aggressive prophylactic embolization or coiling of the gastroduodenal arteries, the right gastric arteries, or other vessels in the hepato-fugal direction may be required to prevent any radiation-induced adverse effects [11–13].

Moreover, injection followed by scintigraphic Tc-MAA scanning may demonstrate significant portal-venous shunting as a contraindication for RE treatment. Radiation pneumonitis has been reported to occur when significant portal-venous shunting is present. Tc-MAA scintigraphy also serves as a method to calculate the required radioactivity of Y-90 for RE therapy.

We have learned from our study that C-arm CT images help to detect or exclude extrahepatic accumulations of contrast material more precisely than DSA alone (Figs. 2, 3). C-arm CT was compared with Tc-MAA for the detection of extrahepatic shunting in a study by Heusner et al. In a cohort of 30 patients, the investigators reported sensitivity, specificity, positive predictive value, negative predictive value,

and accuracy values of 60, 96, 75, 92, and 90%, respectively [14].

C-arm CT is also able to provide more detailed information about tumor vascularity and from which arteries the tumors are deriving their vascular supply (Figs. 4, 5). Loui et al. reported 22 of 42 patients (52%) in whom extrahepatic enhancement or incomplete tumor perfusion was seen on C-arm CT, thus affecting the treatment plan. In 14 patients (33%), the findings were evident exclusively on C-arm CT and were not detected by DSA. This is in agreement with our findings that C-arm CT obtained additional information compared with DSA in 57.4% of patients, thus affecting treatment in 25.5% of patients prepared for RE. When comparing C-arm CT with Tc-MAA scintigraphy, C-arm CT showed eight cases of extrahepatic enhancement (19%) that were not evident on Tc-MAA imaging, according to Loui et al. [15]. Therefore, C-arm CT might have the potential to decrease the risk of therapy-induced complications, thus allowing for more sophisticated therapy planning [16].

Whole-body FDG-PET proved to be useful for comprehensive assessment of intrahepatic and extrahepatic tumor manifestations. Moreover, FDG-PET can also be employed as a baseline scan for the assessment of tumor response to RE [5]. Because PET/CT with venous contrast-phase CT was available in all of our patients during work-up for RE, it also served as the imaging “gold standard” in our study. To our knowledge this is the first study

Fig. 2 Fifty-eight year-old woman with metastases from colorectal cancer. Conventional CT (A) shows a hypodense lesion (*arrowhead*) in segment 6 of the liver, which contains viable tumor tissue as demonstrated by PET. **B** C-arm CT shows typical rim enhancement of the liver metastasis (*arrowhead*) and enhancement of the gall bladder wall (*arrow*). **C** RE with the catheter in this particular location may result in radionecrosis of the gall bladder and cholecystitis unless embolization of the cystic artery is performed

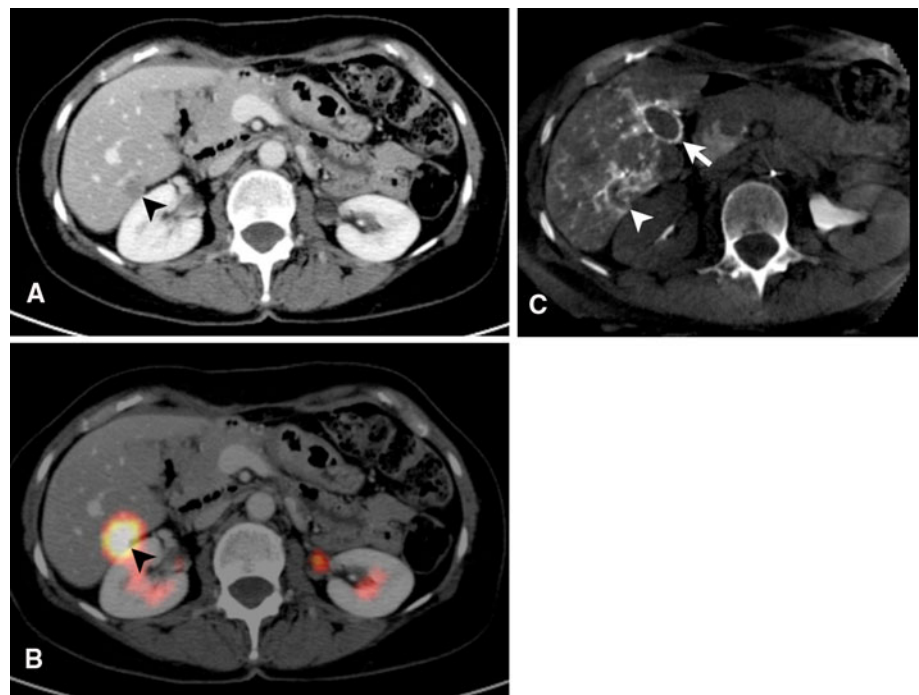


Fig. 3 Fifty-three year-old woman with multifocal liver metastases originating from breast cancer. **A** Tumor blush in the left liver lobe is seen by the central catheter position. A further side branch to the left (*arrowhead*) may lead to extrahepatic or intrahepatic structures in the left upper quadrant. **B** The catheter was retracted, and C-arm CT was performed at this position. **C** C-arm CT images clearly show depicted multifocal liver metastases with rim enhancement. No contrast enhancement is detected outside the liver, e.g., in the stomach (*asterisk*). **D** Venous-phase contrast-enhanced CT at a comparable level displays bright enhancement of the stomach (*asterisk*)

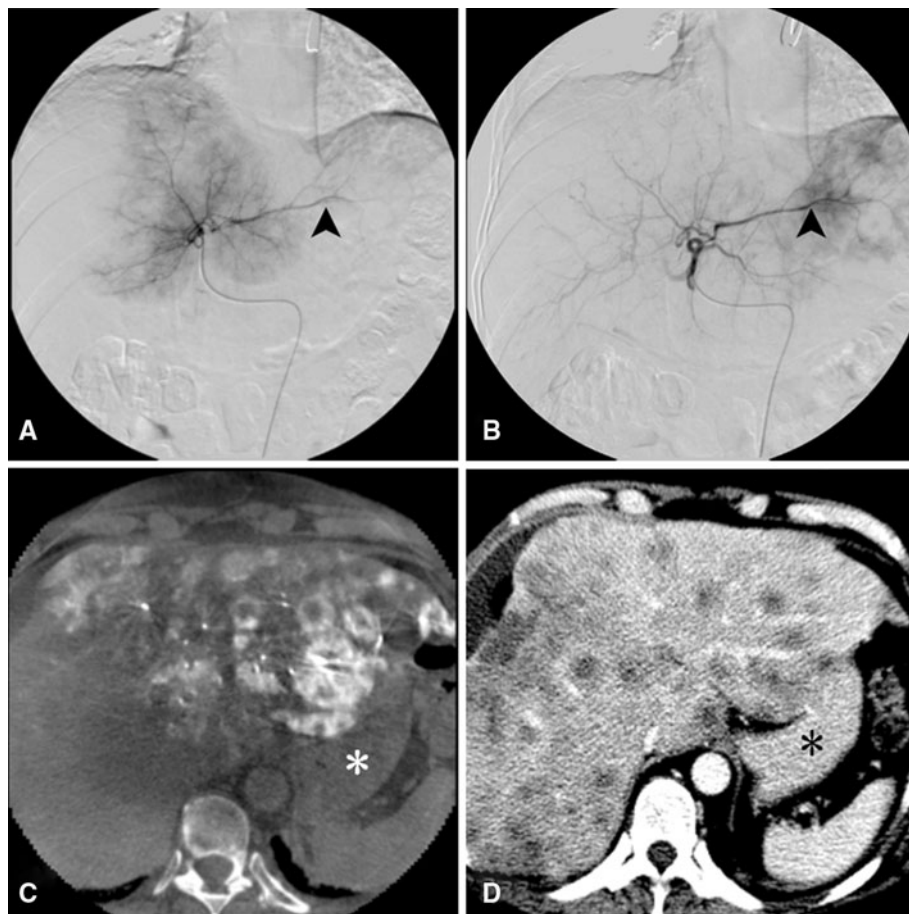


Fig. 4 **A** Sixty-nine year-old woman with cholangiocellular carcinoma presenting as a central mass in the liver. **B** PET/CT shows viable tumor tissue, particularly in the peripheral part of the tumor. **C** C-arm CT image with catheter in the right liver lobe artery shows partial enhancement of the mass. The hypervascularized portion of the tumor as presented by C-arm CT seems to correspond to the viable tumor tissue in PET/CT. Because the tumor was not reached in total from this catheter position, the catheter had to be repositioned to the left liver lobe to complete the therapy

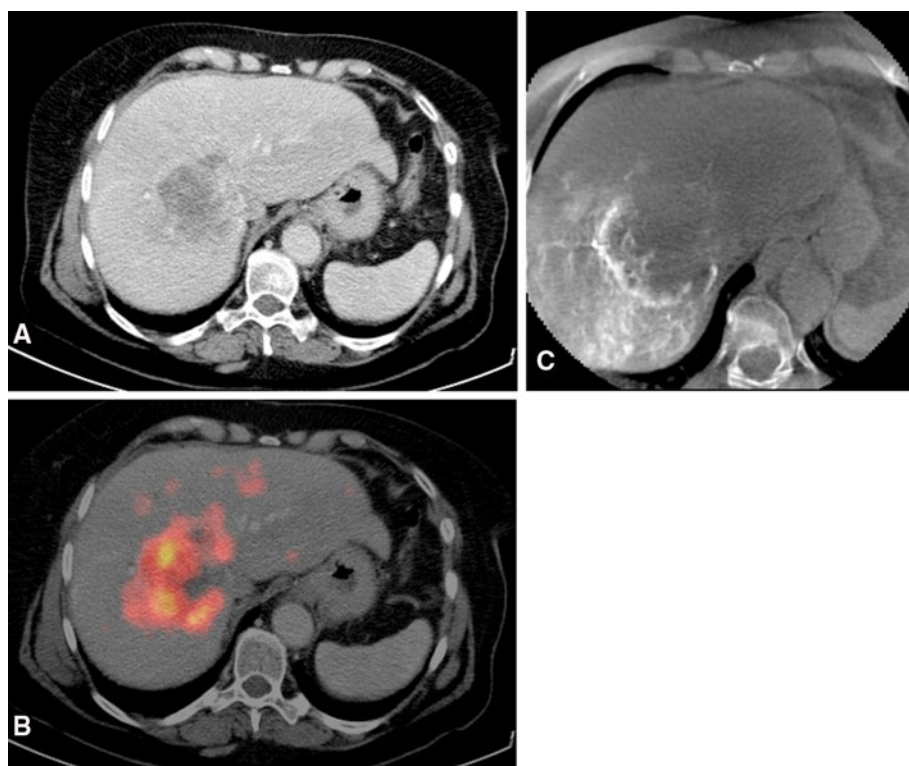
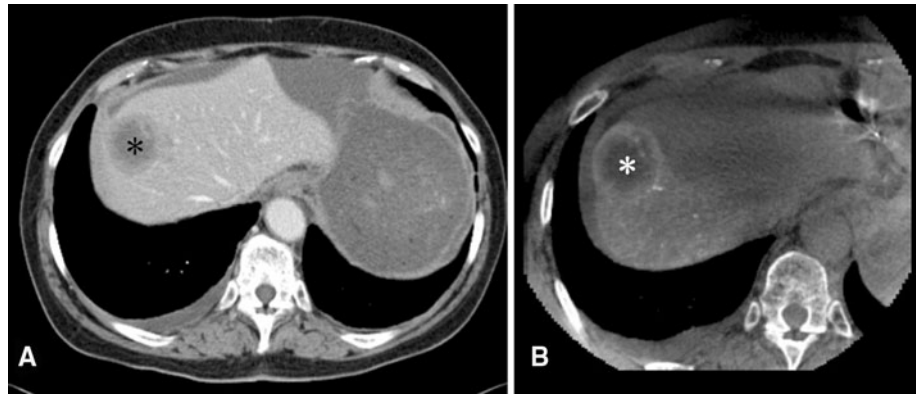


Fig. 5 Seventy-one-year old woman with liver metastasis in segment 8 of the liver. C-arm CT shows that the entire tumor can be reached from the right liver lobe artery



comparing C-arm CT with other imaging modalities, such as conventional venous contrast-phase CT and PET.

Study Limitations

Since we realized that C-arm CT is able to change the decision for RE, we have started to perform this examination in almost all of our patients under consideration for RE. Some patients may be unable to maintain a breath-hold for the 8 seconds required during the C-arm CT run. In the version of C-arm CT imaging we used in this study, the limited field of view may have result in incomplete coverage of the liver and therefore explains the large number of lesions missed by C-arm CT compared with conventional venous contrast-phase CT or PET. A newer version will allow a larger volume to be covered by combining two runs performed with a slight lateral shift and performed one after another. We believe that complete assessment of the liver by C-arm CT has the potential to change determination of eligibility and therapy planning even in a greater number of patients than reported herein [17].

Although it is plausible that the decisions that had been made based on C-arm CT images were appropriate to select patients with different types of cancer for RE, it has not been proven by this study that the criteria were adequate to decrease the incidence of adverse effects related to RE.

We did not measure the additional time required for C-arm CT in addition to DSA, but the procedure can be completed within a few minutes and requires only minor additional time for evaluation. Regarding the decision to either accept or decline a planned RE treatment, C-arm CT images may be analyzed after completion of the diagnostic angiographic examination. It is likely that a better integration of C-arm CT imaging in the angiographic unit will result in seamless integration into the interventional work-flow.

We also did not evaluate radiation exposure associated with C-arm CT runs for both the patient as well as the investigator. Assessment of radiation exposure must be addressed by future research as well as strategies to prevent

scatter radiation to investigators. Set-up scenarios comparable with conventional CT using automated contrast injectors and external triggering of the C-arm CT run may be an alternative to front-side application of contrast media and may thereby prevent investigators from avoidable scatter radiation exposure by C-arm CT.

Conclusion

We found C-arm CT imaging particularly useful for determining the eligibility and feasibility of RE because this procedure requires super-selective approaches and particular precaution for the prevention of adverse effects. As we determined in our study, C-arm CT is not as sensitive as PET and CT for detecting liver tumors and may also not replace Tc-MAA scintigraphy for the detection of shunts. However, this technique is well suited to demonstrate the presence or absence of tumor hypervascularity and to assess whether a particular positioning of the catheter is adequate to target the tumor manifestation to be treated.

Contrast enhancement outside the liver necessitates either relocation of the catheter tip or aggressive coiling of the branch arteries. The detection of various findings with C-arm CT, e.g., arterial- or portal-venous fistulas, may have a pivotal impact on the decision to perform RE.

Disclosure Oliver Meissner and Klaus Klingenberg-Regn are employees of Siemens AG.

Conflict of Interest Statement For all authors no conflict of interest exists.

References

1. Cianni R, Urigo C, Notarianni E et al (2009) Selective internal radiation therapy with SIR-spheres for the treatment of unresectable colorectal hepatic metastases. *Cardiovasc Intervent Radiol* 32:1179–1186

2. Bilbao JI, de Martino A, de Luis E et al (2009) Biocompatibility, inflammatory response, and recanalization characteristics of nonradioactive resin microspheres: histological findings. *Cardiovasc Intervent Radiol* 32:727–736
3. Salem R, Lewandowski R, Sato K et al (2007) Technical aspects of radioembolization with ⁹⁰Y microspheres. *Tech Vasc Interv Radiol* 10:12–29
4. Salem R, Thurston KG (2006) Radioembolization with ⁹⁰Yttrium microspheres: a state-of-the-art brachytherapy treatment for primary and secondary liver malignancies. Part 1: technical and methodologic considerations. *J Vasc Interv Radiol* 17:1251–1278
5. Gulec SA, Fong Y (2007) Yttrium 90 microsphere selective internal radiation treatment of hepatic colorectal metastases. *Arch Surg* 142:675–682
6. Kalender WA, Kyriakou Y (2007) Flat-detector computed tomography (FD-CT). *Eur Radiol* 17:2767–2779
7. Welsh JS, Kennedy AS, Thomadsen B (2006) Selective internal radiation therapy (SIRT) for liver metastases secondary to colorectal adenocarcinoma. *Int J Radiat Oncol Biol Phys* 66:S62–S73
8. Lewandowski RJ, Thurston KG, Goin JE et al (2005) ⁹⁰Y microsphere (TheraSphere) treatment for unresectable colorectal cancer metastases of the liver: Response to treatment at targeted doses of 135–150 Gy as measured by [¹⁸F]fluorodeoxyglucose positron emission tomography and computed tomographic imaging. *J Vasc Interv Radiol* 16:1641–1651
9. Salem R, Lewandowski R, Roberts C et al (2004) Use of Yttrium-90 glass microspheres (TheraSphere) for the treatment of unresectable hepatocellular carcinoma in patients with portal vein thrombosis. *J Vasc Interv Radiol* 15:335–345
10. Bangash AK, Atassi B, Kaklamani V et al (2007) ⁹⁰Y radioembolization of metastatic breast cancer to the liver: toxicity, imaging response, survival. *J Vasc Interv Radiol* 18:621–628
11. Liu DM, Salem R, Bui JT et al (2005) Angiographic considerations in patients undergoing liver-directed therapy. *J Vasc Interv Radiol* 16:911–935
12. Haydar AA, Wasan H, Wilson C, Tait P (2010) ⁹⁰Y radioembolization: embolization of the gastroduodenal artery is not always appropriate. *Cardiovasc Intervent Radiol*. doi:10.1007/s00270-010-9838-6
13. Bilbao JI, Garrastachu P, Herráiz MJ et al (2009) Safety and efficacy assessment of flow redistribution by occlusion of intrahepatic vessels prior to radioembolization in the treatment of liver tumors. *Cardiovasc Intervent Radiol*. doi:10.1007/s00270-009-9717-1
14. Heusner TA, Hamami ME, Ertle J et al (2010) Angiography-based C-arm CT for the assessment of extrahepatic shunting before radioembolization. *Rofo* [Epub ahead of print]
15. Louie JD, Kothary N, Kuo WT et al (2009) Incorporating cone-beam CT into the treatment planning for yttrium-90 radioembolization. *J Vasc Interv Radiol* 20:606–613
16. Murthy R, Mutha P, Madoff DC, Mahvash A, Erwin W (2009) Establishment of the radiation effect of yttrium-90 microspheres: role of C-arm CT. *J Vasc Interv Radiol* 20:422–424
17. Ibrahim SM, Lewandowski RJ, Ryu RK et al (2008) Radiographic response to yttrium-90 radioembolization in anterior versus posterior liver segments. *Cardiovasc Intervent Radiol* 31:1124–1132